Supporting Information

Hierarchical tube brush-like Co_3S_4@NiCo-LDH on Ni foam as bifunctional electrocatalyst for overall water splitting

Xiaohu Xu [a*], Le Su [a], Yujie Zhang [a], Lijuan Dong [b*], Xiangyang Miao [a*]

[a] Key Laboratory of Spectral Measurement and Analysis of Shanxi Province, College of Physics and Information Engineering, Shanxi Normal University, No.1 Gongyuan street, Yaodu District, Linfen 041004, China.

[b] Shanxi Provincial Key Laboratory of Microstructure Electromagnetic Functional Materials, Shanxi Datong University, Xingyun street, Nanjiao District, Datong, 037009, China.

[*]Corresponding author. E-mail: bigbrowm@163.com; Tel:+86-13623578753

[*]Corresponding author. E-mail: donglijuan_2012@163.com; Tel:+86-13994319080

[*]Corresponding author. E-mail: sxxymiao@126.com; Tel:+86-15035757788

Number of pages: 18

Number of figures: 20

Number of tables: 5

Content

Materials

All chemicals in the experiments were purchased at analytical grade and can be used without further purification. Hydrochloric acid, ethanol, sodium sulfide nonahydrate (Na_2S $9H_2O$), nickel nitrate hexahydrate ($Ni(NO_3)_2$ $6H_2O$), cobaltous nitrate hexahydrate ($Co(NO_3)_2$ $6H_2O$), urea ($CO(NH_2)_2$) and potassium hydroxide were purchased from from Sinopharm Chemical Reagent Co., Ltd. Nickel foam (NF) was obtained from the KunShan Kunag Xun Electronics Co., Ltd. Pt/C (20 wt % Pt), ruthenium(IV) oxide (RuO_2) and Nafion (5 wt %) were purchased from Aladdin Ltd. The deionized (DI) water with a resistivity of 18.2 $M\Omega \cdot cm^{-1}$ used in all experiments was purified through a Millipore system.

Fabrication of Pt/C/NF:

For comparison, a benchmark Pt/C electrocatalyst on a NF was fabricated by the following steps: firstly, Pt/C (13.0 mg) and Nafion solution (0.02 mL of 5 wt %) were dispersed in ethanol (0.48 mL). Secondly, the solution underwent sonication for 30 min to form a homogeneous suspension, and then 50 μL of the catalyst ink was dropped on the electrode with a geometrical surface area of 0.2 cm^2. The loading amount is ~6.5 mg cm^{-2}.

Fabrication of RuO_2/NF:

Briefly, 20 mg of RuO_2 and 10 μL of 5 wt % Nafion solution were dispersed in 990 μL of anhydrous ethanol followed by ultrasonication for 20 min to form a catalyst ink. Then 65 μL of catalyst ink was loaded on NF with a geometrical surface area of 0.2 cm^2 and naturally dried. Finally, the RuO_2/NF catalyst was achieved. The mass loading was ~6.5 mg cm^{-2}.

Characterization

The morphology of all samples were investigated by field-emission scanning electron microscopy (FE-SEM, Hitachi, SU-8010) and high-resolution transmission electron microscopy (HR-TEM, JEM-2100, 200 kV) with X-ray energy-dispersive spectroscopy. The crystal diffraction patterns of samples were recorded by X-ray diffractometer (XRD, Bruker D8-Advance) equipped with a Cu Kα radiation source (λ =1.5418 Å). The surface composition and valence state of the samples were characterized by X-ray photoelectron spectroscopy (XPS, Kratos Axis Ultra DLD). Raman characterization was performed on a Renishaw-inVia Raman spectrometer

with 532 nm laser excitation. Fourier transform infrared spectroscopy (FTIR, Nicolet) was used to get the fingerprint of chemical bonding vibration of the material.

Electrochemical measurements

All electrochemical data tests were obtained by an electrochemical workstation (CHI 760E, CH Instruments, China) with a three-electrode cell configuration. The three-electrode cell employed the as-prepared samples supported on Ni foam as the working electrode, a mercury oxide electrode (Hg/HgO) as the reference one, and a carbon rod (4 mm in diameter) as the counter one, respectively. Cyclic Voltammetry (CV) measurements were conducted for OER and HER at the potential ranging from 0 to 1 V (vs. Hg/HgO), -1.5 to -1 V (vs. Hg/HgO) at a scan rate of 200 mV s^{-1}, respectively. Polarization curves for OER and HER were obtained using Linear Sweep Voltammetry (LSV) with a scan rate of 3 and 5 mV s^{-1} in an O_2 saturated 1.0 M KOH, respectively. When the signals of working electrodes stabilized after scanning several times, the data were collected. Electrochemical impedance spectroscopy (EIS) experiments were performed in the frequency range from 100 KHz to 1 Hz with an amplitude potential of 5 mV. The stability test was implemented using chronopotentiometric method at certain potentials. All the potentials with regard to Hg/HgO, reported in this work, were converted to the reversible hydrogen electrode (RHE) according to the following equation: E (RHE) = E (vs. Hg/HgO) + 0.059 × pH+ 0.098. All the measurements above were corrected by manual iR compensation using the current and the solution resistance.

Effect of urea during the hydrothermal reaction

Urea, as a common surfactant, can control the precipitation of cations by generating hydroxide ions in solution slowly through mild hydrolysis. Meanwhile, the surfactant effects of urea hydrolysis have been used to assist the synthesis of crystals with particular morphologies, such as nanosheets, nanowires, nanoflowers and so on. Thus, in order to obtain the target morphology of the catalysts, urea was added in the first and third steps of the hydrothermal reaction under different temperature. In addition, the adding of urea also affects the catalytic performance towards HER and OER of the final hydrothermal sample. In order to verify the above statement, we also conducted three sets of comparison experiments to compare the crystal phase, morphology of the hydrothermal product and the corresponding catalytic performances in the absence/presence of urea, which are displayed in the following. As can be seen from the Fig.S1 and R2, the addition of urea not only affect the crystal phase of hydrothermal samples but also changes the corresponding morphology of as-prepared samples. Meanwhile, the catalytic activity of CoCHH/NF and Co_3S_4@NiCo-LDH/NF is more or less improved for both HER and OER in the presence of urea as shown in Fig.S3, which may be attributed to the difference of morphology of the samples after adding urea. To sum up, urea was chosen to add during the hydrothermal process.

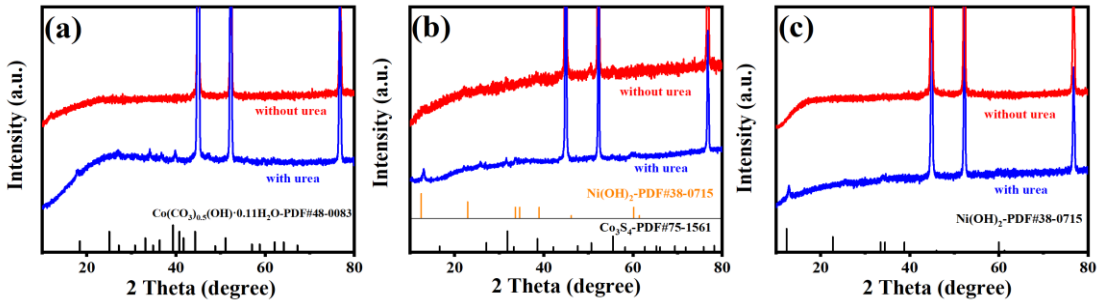

Fig. S1 XRD patterns of products obtained in the absence/presence of urea: (a) CoCHH/NF; (b) Co_3S_4@NiCo-LDH/NF; (c) NiCo-LDH/NF.

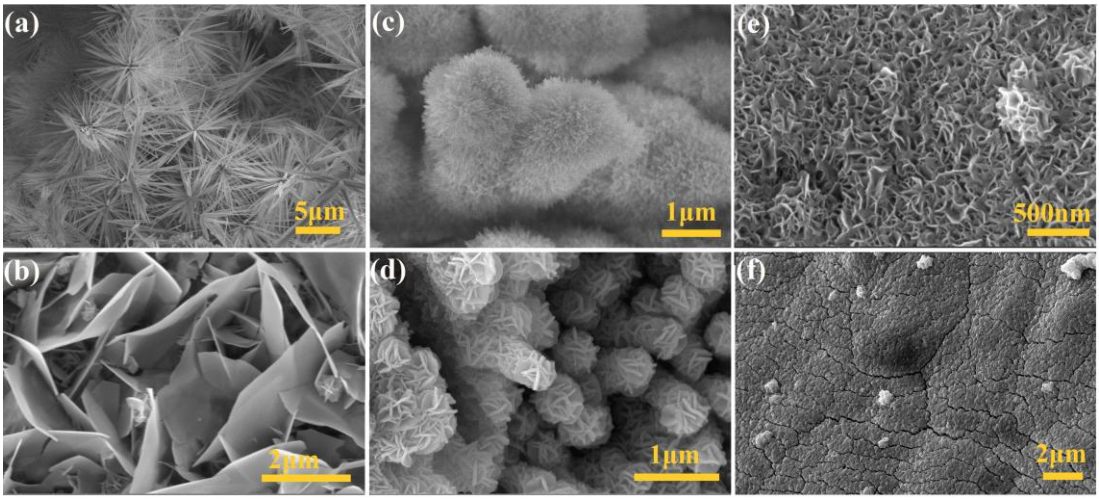

Fig. S2 FE-SEM images of products obtained in the absence (bottom)/presence (top) of urea: (a, b) CoCHH/NF; (c, d) Co_3S_4@NiCo-LDH/NF; (e, f) NiCo-LDH/NF.

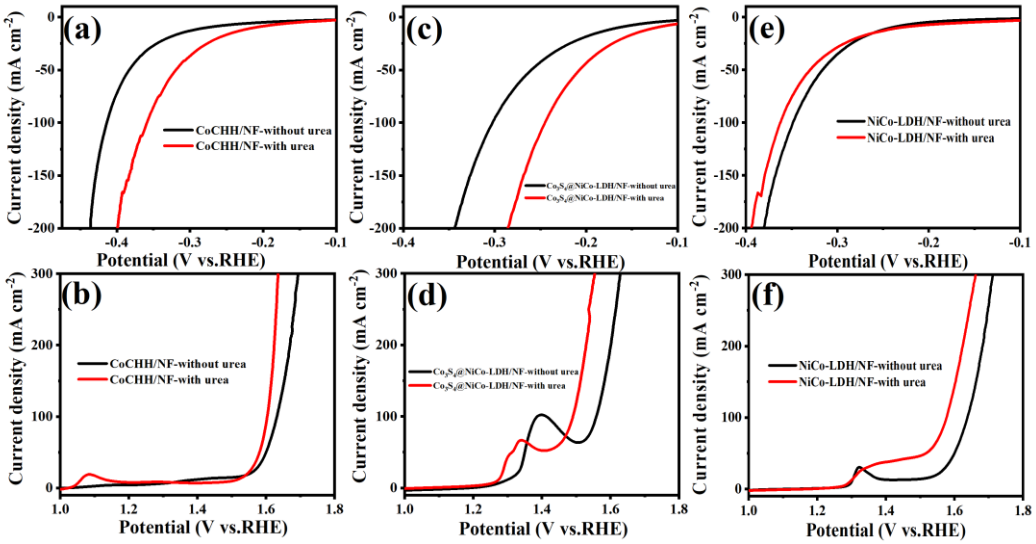

Fig. S3 Polarization curves for HER and OER in the absence/presence of urea: (a, b) CoCHH/NF; (c, d) Co_3S_4@NiCo-LDH/NF; (e, f) NiCo-LDH/NF.

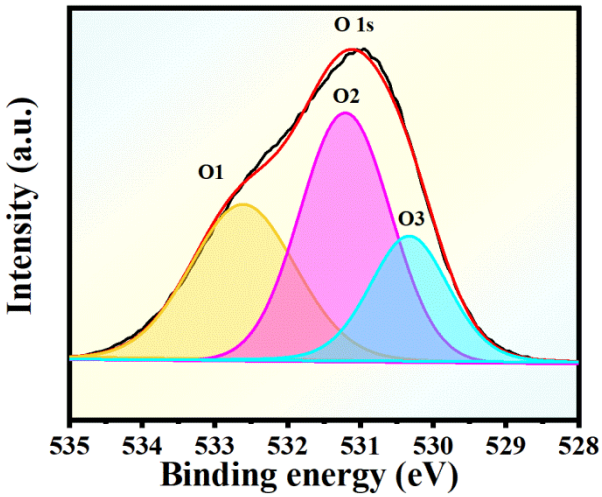

Fig. S4. High-resolution XPS spectrum of O 1s for Co_3S_4@NiCo-LDH.

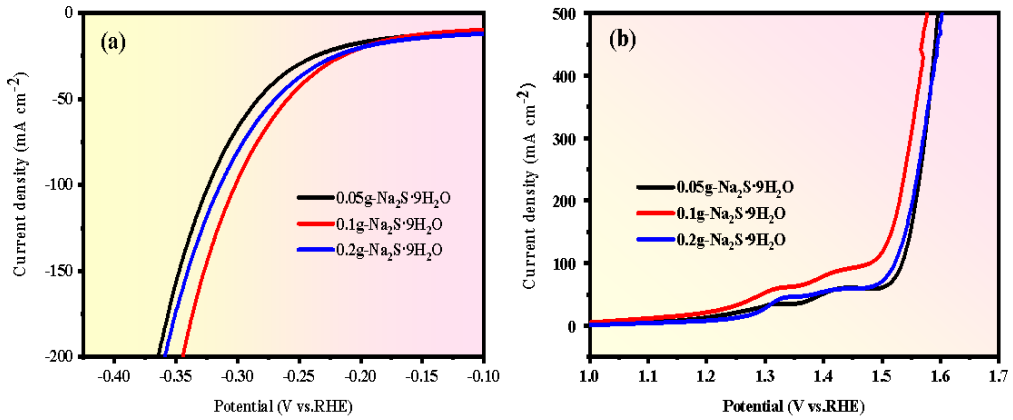

Fig. S5. (a) HER polarization curves and (b) OER polarization curves of Co_3S_4/NF samples synthesized with different amounts of Na_2S $9H_2O$.

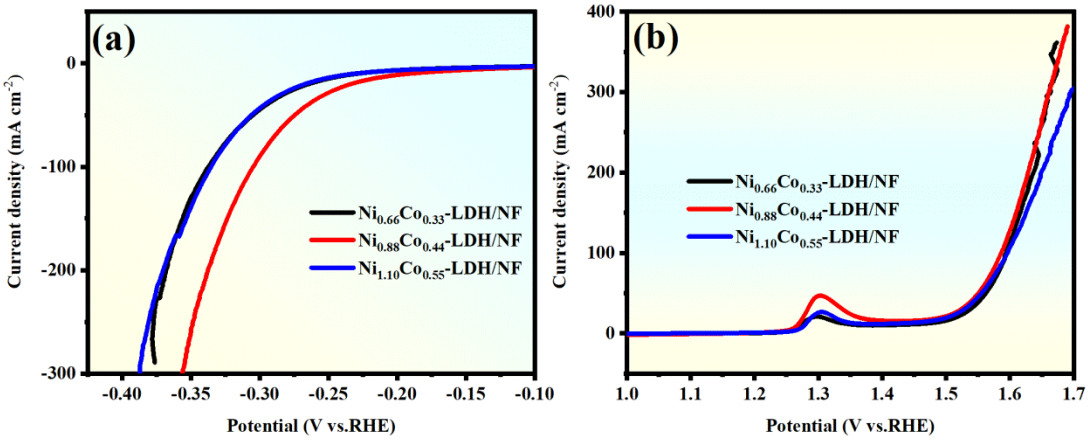

Fig. S6. (a) HER polarization curves and (b) OER polarization curves of NiCo-LDH/NF samples synthesized with different amounts of $Co(NO_3)_2$ $6H_2O$ and $Ni(NO_3)_2$ $6H_2O$.

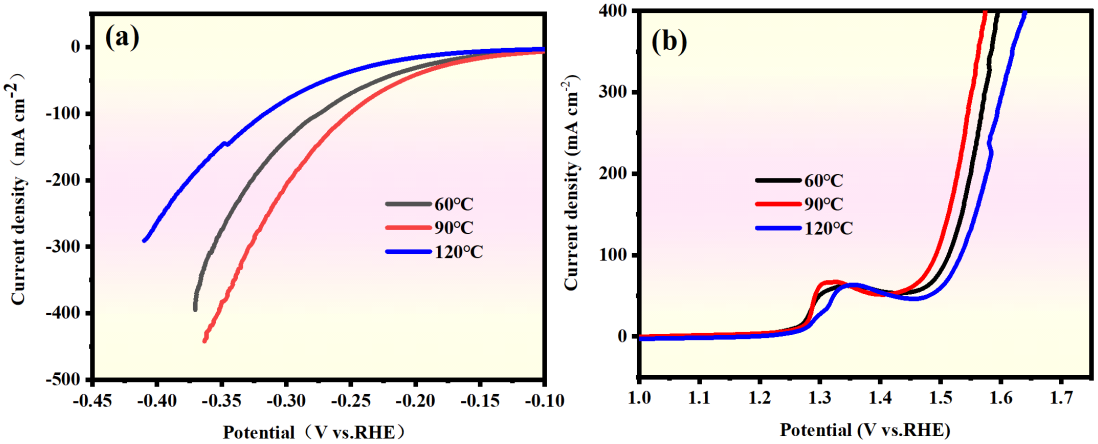

Fig. S7. (a) HER polarization curves and (b) OER polarization curves of Co_3S_4@NiCo-LDH/NF samples synthesized by different hydrothermal temperature.

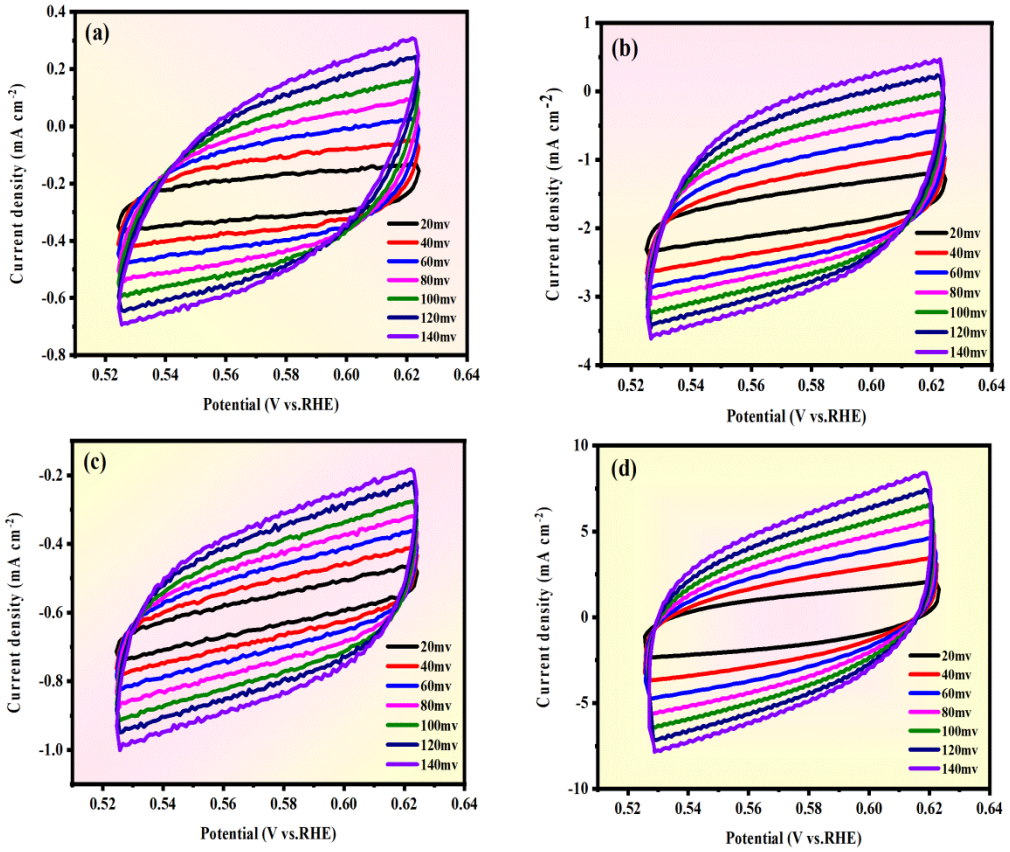

Fig. S8. CV curves of (a) NF, (b) Co_3S_4/NF, (c) NiCo-LDH/NF, (d) Co_3S_4@NiCo-LDH/NF in the non-faradaic region with different scanning rates from 20 to 140 mV s^{-1}.

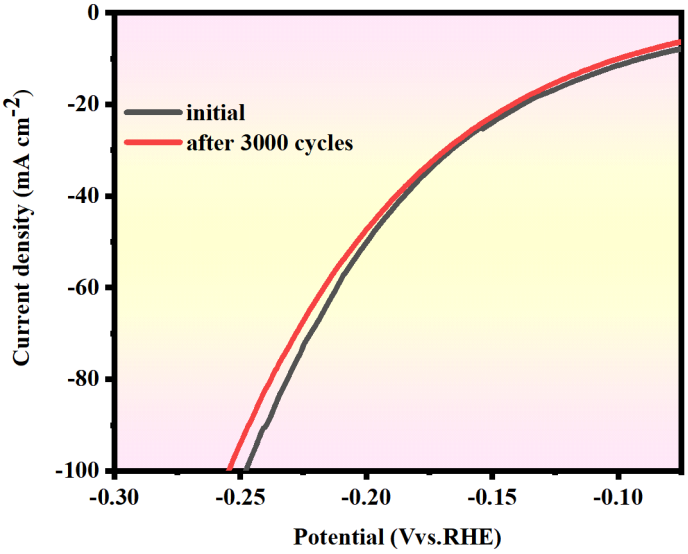

Fig. S9. LSV curves of Co_3S_4@NiCo-LDH/NF before and after 3000 cycles.

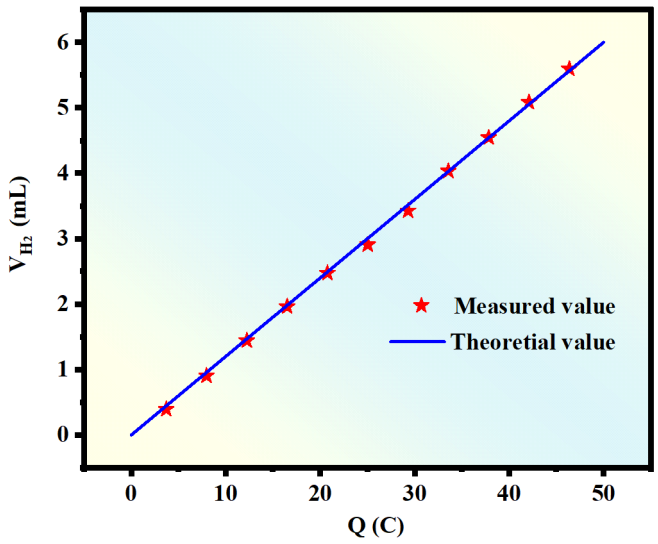

Fig. S10. Quantitative H_2 measurement via water displacement.

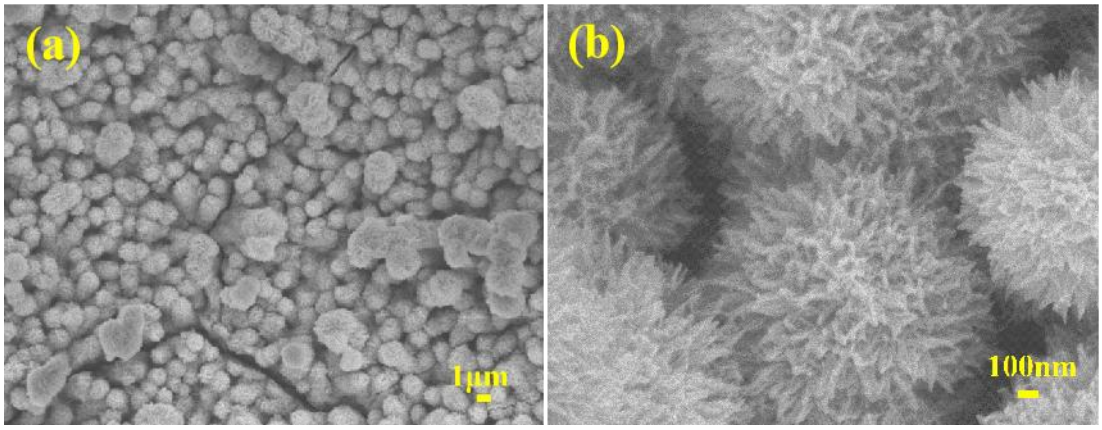

Fig. S11. Representative FE-SEM images of the Co_3S_4@NiCo-LDH/NF catalyst after continuous 20 h for HER.

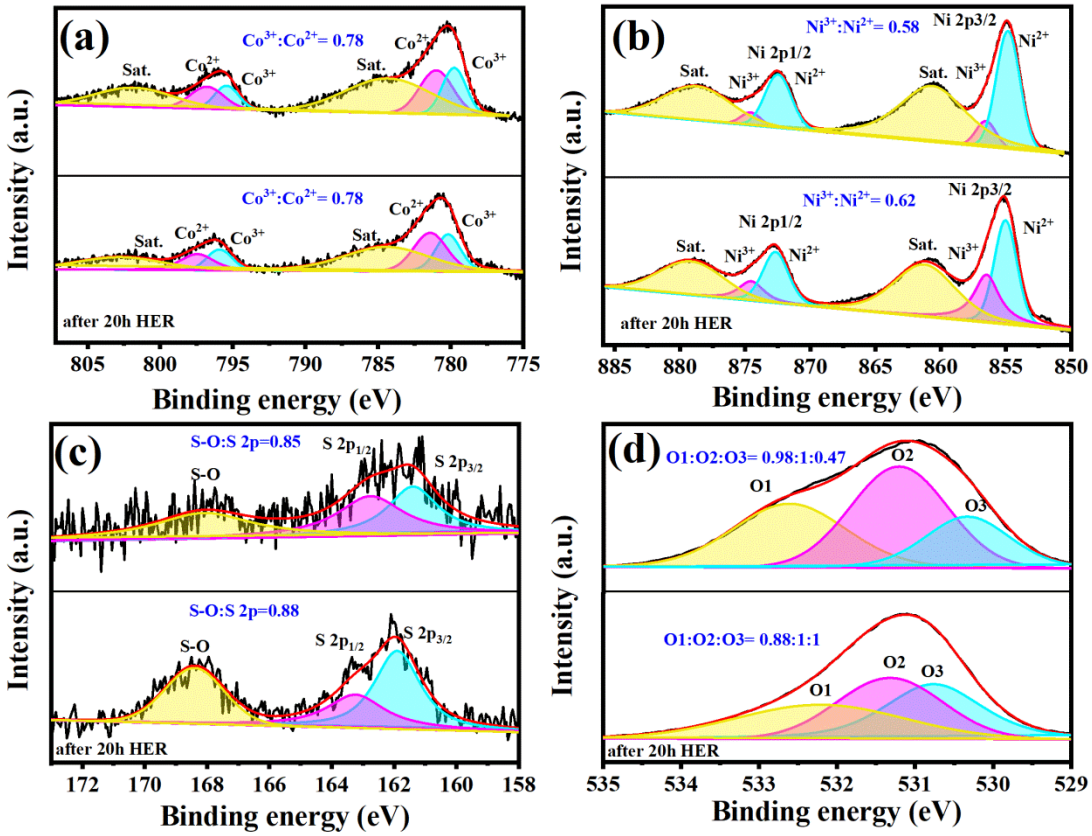

Fig. S12. (a) XPS full survey spectrum of Co_3S_4@NiCo-LDH/NF after continuous 20 h HER electrolysis. High-resolution XPS spectrum: (b) Co 2p, (c) Ni 2p, and (d) S 2p.

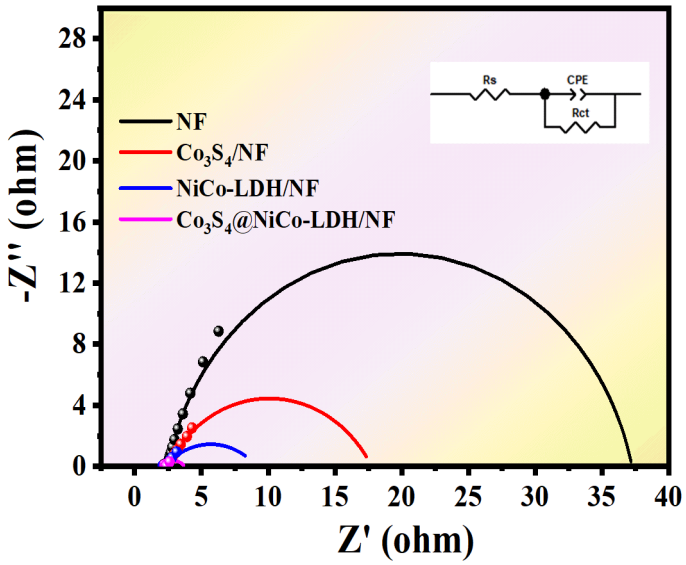

Fig. S13. Nyquist plot of the NF, NiCo-LDH/NF, Co_3S_4/NF, Co_3S_4@NiCo-LDH/NF catalysts at overpotential of 100 mV vs. RHE.

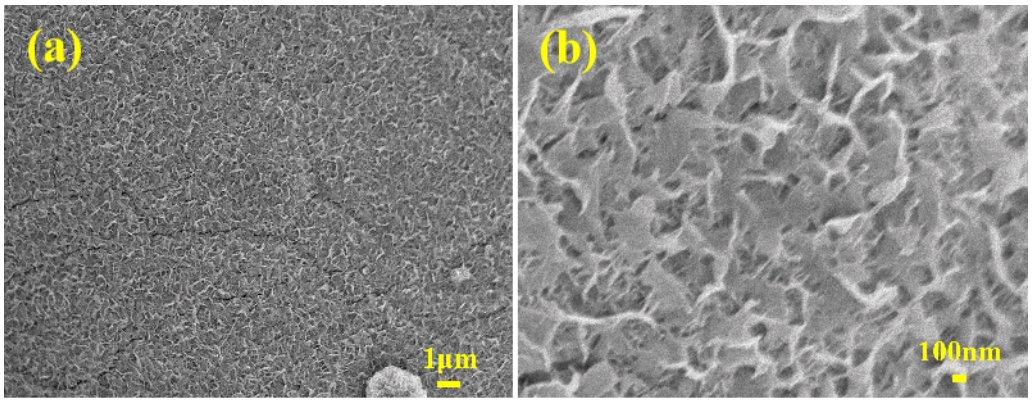

Fig. S14. Representative FE-SEM images of the Co_3S_4@NiCo-LDH/NF catalyst after continuous 20 h at 10 mA cm^{-2} for OER.

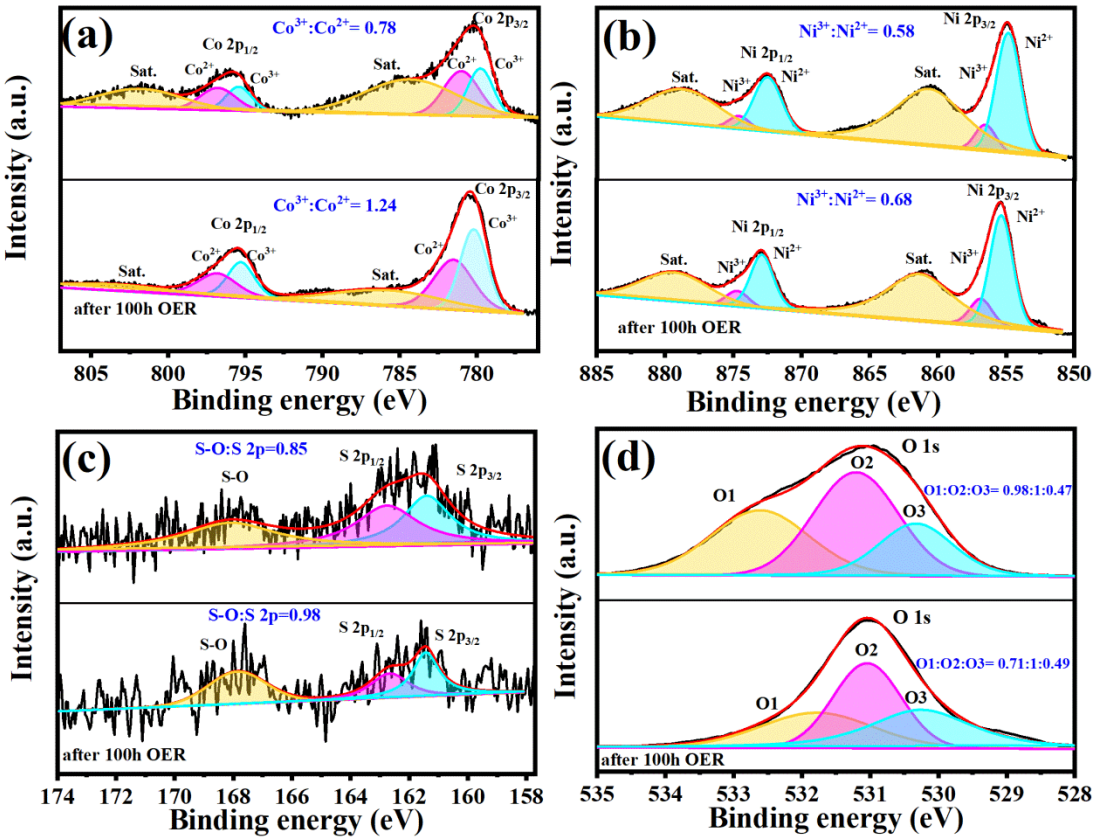

Fig. S15. (a) XPS full survey spectrum of Co_3S_4@NiCo-LDH/NF after OER test for 20 h. High-resolution XPS spectrum: (b) Co 2p, (c) Ni 2p, and (d) S 2p.

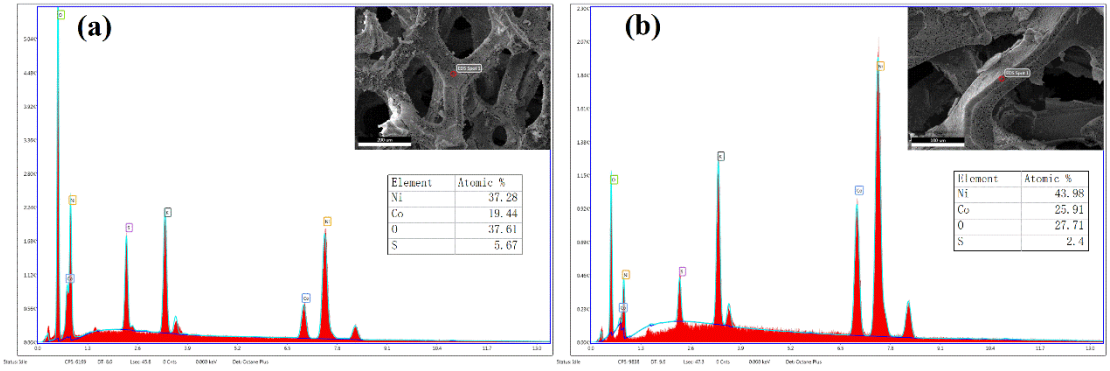

Fig. S16 EDX pattern of Co_3S_4@NiCo-LDH/NF before and after OER stability test at 100 mA cm^{-2} for 20 h.

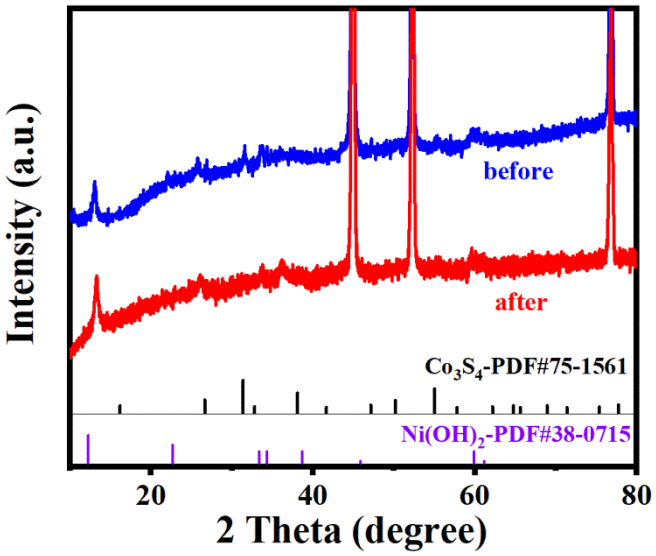

Fig. S17 XRD patterns of Co_3S_4@NiCo-LDH/NF before and after OER stability test at 100 mA cm^{-2} for 20 h.

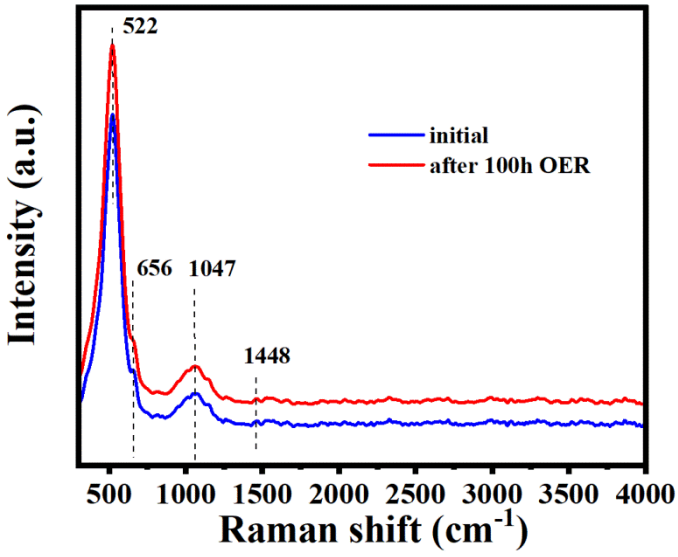

Fig. S18 Raman spectra of Co_3S_4@NiCo-LDH//NF before and after OER stability test at 100 mA cm^{-2} for 100 h.

The observed peaks at 522 and 656 cm^{-1} can be assigned to Co_3S_4, and the peaks at 1047 and 1448 cm^{-1} are ascribed to NiCo-LDH.

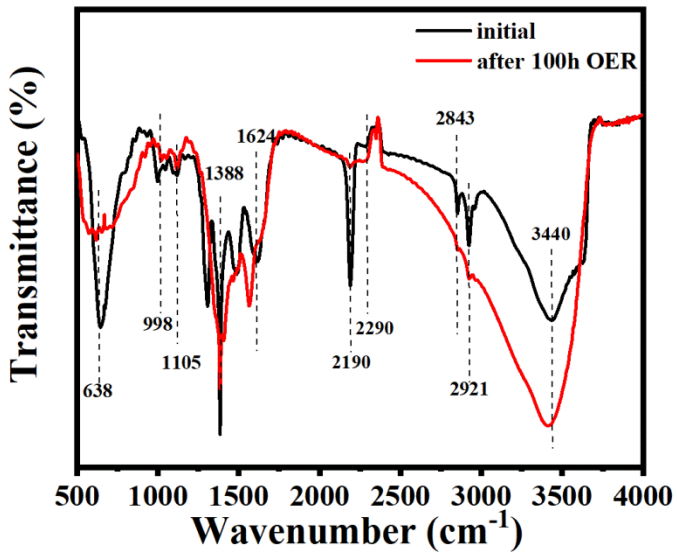

Fig. S19 FTIR spectra of Co_3S_4@NiCo-LDH//NF before and after OER stability test at 100 mA cm^{-2} for 100 h.

FT-IR spectroscopy studies of the Co_3S_4@NiCo-LDH/NF before and after OER stability test are carried out separately to provide a fingerprint of molecular vibrations and identify the characteristic functional group of the as-prepared samples in Figure R10. The broad band at around 3440 and 1624 cm^{-1} is ascribed to the stretching and bending vibrations of OH. The absorption bands displayed at 638, 998 and 1105 cm^{-1} were attributed to the stretching vibrations of M-O, M-O-M and O-M-O (M = Ni and Co). The sharp bands at 2843 and 2921 cm^{-1} were related to the ν_{C-O} and ν_{C-H} vibration modes.

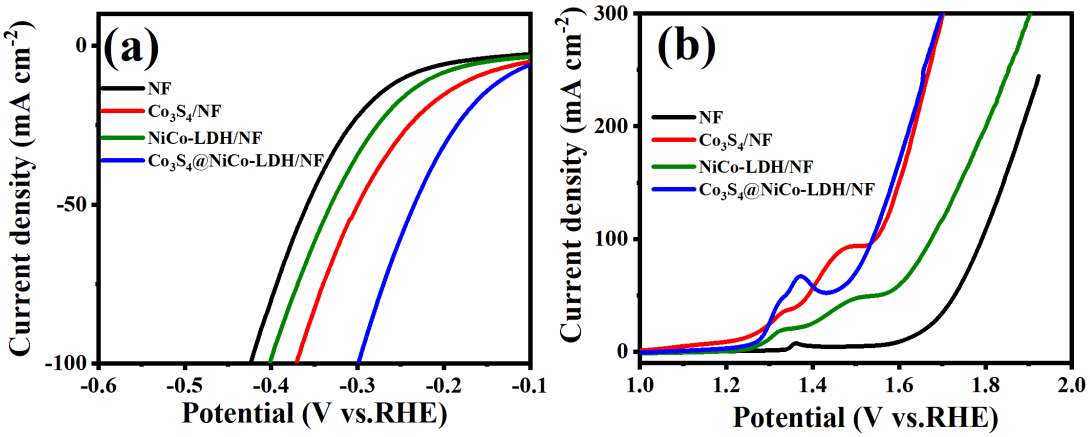

Fig. S20 Polarization curves without iR compensation of all samples towards: (a) HER and (b) OER, respectively.

Table. S1. Comparisons of HER catalytic activity of Co_3S_4@NiCo-LDH with some previous reported catalysts in 1 mol/L KOH solution.

Catalyst	Substrate	Overpotential (mV) @ j=10 mA cm^{-2}	Reference
Co_3S_4@NiCo-LDH	Ni foam	125	This work
$NiCo_2O_4$/FeNi-LDH	Ni foam	192	[1]
$Co_{0.85}Se$/FeNi-LDH	Ni foam	260	[2]
$NiCo_2S_4$/NiFe-LDH	Ni foam	200	[3]
CoS_2	Carbon cloth	193	[4]
NiCo-LDH	Ni foam	162	[5]
Co_9S_8@NiCo-LDH	Ni foam	168	[6]
$FeCo_2S_4$@CoFe-LDH	Ni foam	115	[7]
CuO@CoZn-LDH	Cu foam	124	[8]
NiFe-LDH@NiCoP	Ni foam	120	[9]
Co_3O_4@NiFe-LDH	Ni foam	74	[10]
NiFe-LDH@Ni_3S_2	Ni foam	184	[11]
Ni_3Se_4@NiFe-LDH	carbon fiber cloth	85	[12]
$CoNi_2S_4$@NiMn LDH	carbon cloth	82	[13]
$CoCO_3$@NiFe-LDH	Ni foam	171	[14]
Ni_3N-NiMoN	carbon cloth	31	[15]

$Mo_xW_{1-x}S_2@Ni_3S_2$	Ni foam	98	[16]

Table. S2. EIS parameters of different samples for HER.

Electrode	R_s (Ω)	R_{CT} (Ω)
Ni foam	2.59	33.51
NiCo-LDH/NF	2.74	14.09
Co_3S_4/NF	2.58	10.68
Co_3S_4@NiCo-LDH/NF	2.53	2.30

Table. S3. EIS parameters of different samples for OER.

Electrode	R_s (Ω)	R_{CT} (Ω)
Ni foam	2.44	34.79
NiCo-LDH/NF	2.25	6.87
Co_3S_4/NF	2.42	15.33
Co_3S_4@NiCo-LDH/NF	2.33	1.37

Table. S4. Comparison of OER catalytic performance of Co_3S_4@NiCo-LDH/NF with other recently reported non-precious metal electrocatalysts in 1 mol/L KOH solution.

Catalyst	Substrate	Overpotential (mV) @ j mA cm^{-2}	Reference
Co_3S_4@NiCo-LDH	Ni foam	262 @ 100	This work
$NiCo_2O_4$/FeNi-LDH	Ni foam	290 @ 50	[1]
CoS_2	Carbon cloth	~350 @ 100 276 @ 10	[4]
NiCo-LDH	Ni foam	~370 @ 100 271 @ 10	[5]
Co_9S_8@NiCo-LDH	Ni foam	330 @ 100	[6]
$FeCo_2S_4$@CoFe-LDH	Ni foam	259 @ 100	[7]
CuO@CoZn-LDH	Cu foam	279 @ 100	[8]
Co_3O_4@NiFe-LDH	Ni foam	269 @ 100	[10]
NiFe-LDH@Ni_3S_2	Ni foam	~420 @ 100 271 @ 20	[11]
Ni_3Se_4@NiFe-LDH	carbon fiber cloth	~280 @ 100 223 @ 10	[12]
$CoNi_2S_4$@NiMn LDH	carbon cloth	269 @ 100	[13]
$CoCO_3$@NiFe-LDH	Ni foam	~380 @ 100 232 @ 20	[14]

$Mo_xW_{1-x}S_2@Ni_3S_2$	Ni foam	～360 @ 100 285 @ 10	[16]

Table S5. Comparison cell voltage of hierarchical Co_3S_4@NiCo-LDH/NF with other bifunctional electrocatalysts in 1 mol/L KOH solution.

Catalyst	Substrate	cell voltage (V) @ j=10 mA cm^{-2}	Reference
Co_3S_4@NiCo-LDH	Ni foam	1.59	This work
$NiCo_2O_4$/FeNi-LDH	Ni foam	1.6	[1]
$Co_{0.85}Se$/FeNi-LDH	graphene foil	1.67	[2]
$NiCo_2S_4$/NiFe-LDH	Ni foam	1.6	[3]
CoS_2	Carbon cloth	1.67	[4]
NiCo-LDH	Ni foam	1.66	[5]
Co_9S_8@NiCo-LDH	Ni foam	1.63	[6]
$FeCo_2S_4$@CoFe-LDH	Ni foam	1.6	[7]
CuO@CoZn-LDH	Cu foam	1.55	[8]
NiFe-LDH@NiCoP	Ni foam	1.57	[9]
Co_3O_4@NiFe LDH	Ni foam	1.56	[10]
NiFe-LDH@Ni_3S_2	Ni foam	1.65	[11]
Ni_3Se_4@NiFe LDH	carbon fiber cloth	1.54	[12]
$CoNi_2S_4$@NiMn LDH	carbon cloth	1.5	[13]
$CoCO_3$@NiFe-LDH	Ni foam	1.67	[14]
Ni_3N-NiMoN	carbon cloth	1.54	[15]
$Mo_xW_{1-x}S_2@Ni_3S_2$	Ni foam	1.62	[16]

References

(1) Z. Wang, S. Zeng, W. Liu, X. Wang, Q. Li, Z. Zhao and F. Geng, *ACS Appl. Mater. Inter.*, 2017**, 9** (2), 1488-1495.

(2) Y. Hou, M. R. Lohe, J. Zhang, S. Liu, X. Zhuang and X. Feng, *Energ. Environ.*

Sci., 2016**, 9** (2), 478-483.

(3) J. Liu, J. Wang, B. Zhang, Y. Ruan , L. Lv, X. Ji , K. Xu , L. Miao and J. Jiang, *ACS Appl. Mater. Inter.*, 2017**, 9** (18), 15364-15372.

(4) C. Guan, X. Liu, A. M. Elshahawy, H. Zhang, H. Wu, S. J. Pennycook and J. Wang, *Nanoscale Horiz.*, 2017**, 2** (6), 342-348.

(5) W. Liu, J. Bao, M. Guan, Y. Zhao, J. Lian, J. Qiu, L. Xu, Y. Huang, J. Qian and H. Li, *Dalton T.*, 2017**, 46** (26), 8372-8376.

(6) J. Yan, L. Chen and X. Liang, Sci. Bull., 2019**, 64** (3), 158-165.

(7) Y. Huang, X. Chen, S. Ge, Q. Zhang, X. Zhang, W. Li and Y. Cui, Catal. Sci. Technol., 2020**, 10** (5), 1292-1298.

(8) L. Yin, X. Du, C. Di, M. Wang, K. Su and Z. Li, *Chem.Eng. J.*, 2021, **414** (15), 128809.

(9) H. Zhang, X. Li, A. Hänel, V. Naumann, C. Lin, S. Azimi, S. L. Schweizer, A. W. Maijenburg and R. B. Wehrspohn, *Adv. Funct. Mater.*, 2018**, 28** (14), 1706847.

(10) S. Wang, J. Wu, J. Yin, Q. Hu, D. Geng and L.-M. Liu, *ChemElectroChem*, 2018**, 5** (10), 1357-1363.

(11) X. Liang, Y. Li, H. Fan, S. Deng, X. Zhao, M. Chen, G. Pan, Q. Xiong and X. Xia, *Nanotechnology*, 2019**, 30** (48), 484001.

(12) T. Zhang, L. Hang, Y. Sun, D. Men, X. Li, L. Wen, X. Lyu and Y. Li, *Nanoscale Horiz.*, 2019**, 4** (5), 1132-1138.

(13) P. Wang, J. Qi, C. Li, W. Li, T. Wang and C. Liang, *Electrochim. Acta*, 2020**, 345**, 136247.

(14) R. Que, S. Liu, P. He, Y. Yang and Y. Pan, *Mater. Lett.*, 2020**, 277**, 128285.

(15) A. Wu, Y. Xie, H. Ma, C. Tian, Y. Gu, H. Yan, X. Zhang, G. Yang and H. Fu, *Nano Energy*, 2018**, 44**, 353-363.

(16) M. Zheng, J. Du, B. Hou and C. L. Xu, *ACS Appl. Mater. Inter.*, 2017**, 9** (31), 26066-26076.